Two cycles deformation effects on NiTi pseudoelastic alloy microstructure

V. Di Cocco, L. Tomassi
DiMSAT , University of Cassino, via G. Di Biasio 43, 03043, Cassino (FR), Italy.
v.dicocco@unicas.it

C. Maletta
Dip. of Mechanical Engineering, University of Calabria, 87036 Rende (CS), Italy.

S. Natali
D.I.C.M.A., University of Rome "Sapienza", via Eudossiana 18, 00185 Rome, Italy.

ABSTRACT. Thanks to their special functional properties, such as pseudo–elasticity or shape memory effect, NiTi alloys are more and more used in various fields. NiTi alloys are also characterized by high mechanical performances and high resistance to corrosion in many aggressive environments in presence of Cl^- such as sea environments or biological environments. Shape memory effect or pseudoelastic effect are due to structural changes in presence of imposed deformation and/or temperature effects. In this work two NiTi alloy, once with a pseudo-elastic behavior and once with shape memory effect are investigated. Single cycle of load-unload for each alloy was effectuated on mini-specimens that allows X-ray analyses under imposed deformation. The results have been compared with those obtained after complete unload conditions.

SOMMARIO. Le leghe a memoria di forma costituite da nickel e da titanio sono sempre più utilizzate in molti ambiti grazie alle loro caratteristiche di recupero della forma. Sono due gli effetti principali delle leghe NiTi, l'effetto del recupero della forma a seguito di un riscaldamento della lega, ed il recupero della forma a seguito della cessazione del carico applicato. Nel primo caso si parla di leghe a memoria di forma, nel secondo di leghe dal comportamento pseudo-elastico. In questo lavoro vengono studiati gli effetti sulla struttura di due leghe NiTi a memoria di forma ed a comportamento pseudo elastico a seguito di un ciclo di carico-scarico.

KEYWORDS. Shape Memory alloys; Pseudo-elastic behaviors; Stress-induced martensitic transformation; X-Ray analyses.

INTRODUCTION

Shape memory effect (SME) and pseudo-elastic effect (PE) are two of most important features with respect to common engineering alloys, of many near equiatomic NiTi alloys. Both shape memory alloys (SMA) and pseudo-elastic alloys (PEA) are able to recover their original shape after high mechanical deformations, the first ones by heating up to characteristic temperature (SME), and the second ones simply by removing the mechanical load (PE). Many kinds of shape memory alloys have been exploited in the last decades, such as the copper-zinc-aluminum (ZnCuAl), copper-aluminum-nickel (CuAlNi), nickel-manganese-gallium (NiMnGa), nickel-titanium (NiTi), and other SMAs created by alloying zinc, copper, gold, iron, etc., but the near equiatomic NiTi binary system shows the most exploitable

characteristics and it is currently used in an increasing number of applications in many fields of engineering [1], for the realization of smart sensors and actuators, joining devices, hydraulic and pneumatic valves, release/separation systems, consumer applications and commercial gadgets. Furthermore wide fields are open to formulate models to predict the behavior of SMAs applied to the real common object such as spring deformation actuated by SMA springs [2]. Another important field of NiTi application is the medicine, due to their good biocompatibility, where the pseudo-elasticity is mainly exploited for the realization of several components such as cardiovascular stent, embolic protection filters, orthopedic components, orthodontic wires, micro surgical and endoscopic devices.
From the microstructural point of view shape memory and pseudo-elastic effects are due to a reversible solid state microstructural transitions from austenite to martensite, which can be activated by mechanical and/or thermal loads [3].
The phase transition of near equiatomic NiTi systems is illustrated in the phase diagram of Fig. 1, where at T<900°C complete temperature transformations are not well specified. Other phase transformations / transitions are observed in the last year, but they are yet not be well understood [4-10].

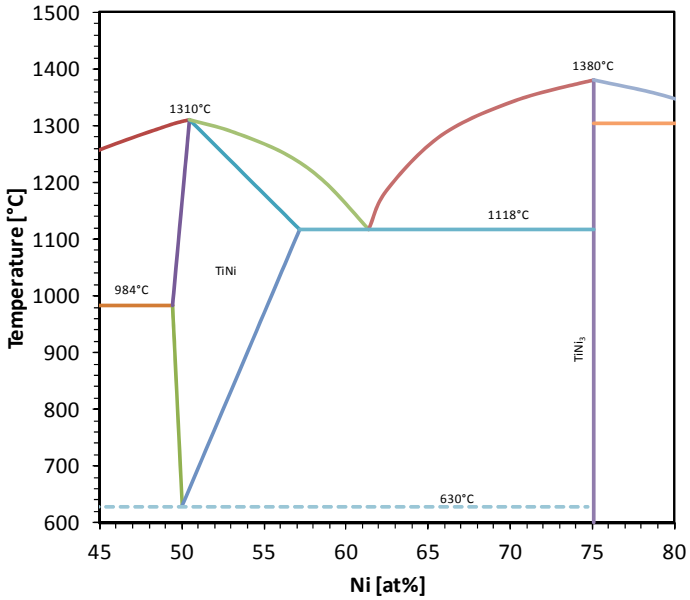

Figure 1: NiTi alloy phase diagram.

The near equiatomic NiTi system is capable of two successive martensitic phase transformations during cooling from its high temperature austenitic phase due to thermo-elasticity and twin deformations in NiTi alloy facilitating shape memory effect (SME) [11-13]. For these reason the traditional microstructure analyses are not well suitable, as showed in the literature where has been showed the influence of mechanical interaction during preparation on microstructure [13]. Furthermore studies showed that presence of needle-like structures founded after etching with concentrated HF containing solutions are not martensitic but austenitic phases characterized by an abnormal aspect [14].
In this work the mechanical properties of a commercial NiTi shape memory alloy have been investigated by tensile tests of miniaturized dog bone shaped specimens carried out by using a mini testing machine. In addition, *in situ* XRD analyses were performed during mechanical tests.

MATERIAL AND METHODS

In this work a commercial pseudo-elastic NiTi alloy (Type S, Memory metalle, Germany), with nominal chemical composition of 50.8at.% Ni - 49.2 at.% Ti, was used to investigate the evolution of microstructure during two loading-unloading cycles.
The engineering stress-strain curve of the material is illustrated in Fig 2, together with the values of the main mechanical parameters of the alloy, *i.e.* the Young's moduli of austenite (E_A) and martensite (E_M), the uniaxial transformation stress (σ^{tr}) and transformation strain (ε_L). The curve was obtained from an isothermal tensile test, carried out at room

temperature (T=298 K) by using a servo hydraulic universal testing machine, equipped with an electrical extensometer with a gauge length of 10 mm to measure the engineering deformations of standard dog-bone shaped specimen.

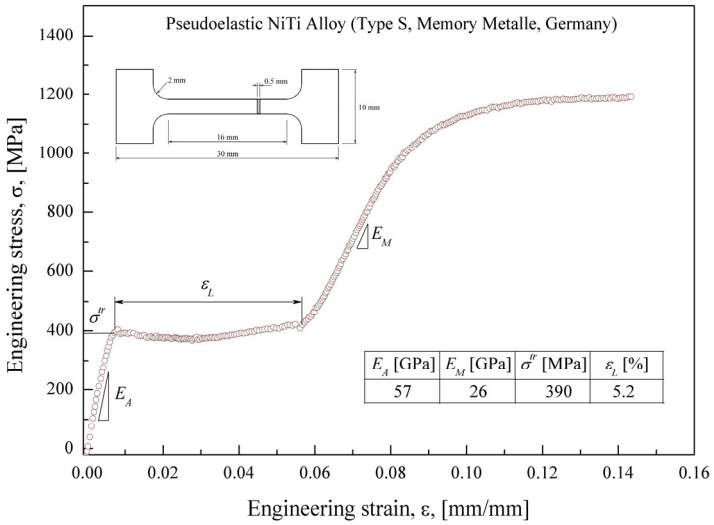

Figure 2: Isothermal stress-strain curve of the investigated alloy carried out at room temperature (T=298k).

The evolution of the microstructure during uniaxial deformation was analyzed by a miniature testing machine which allows *in-situ* scanning electron microscopic (SEM) observations as well as X-Ray micro-diffraction analyses. In particular, the testing machine is equipped with a simple and removable loading frame, which allows SEM and X-Ray analyses at fixed values of applied load and/or deformations. The machine is powered by a stepping motor, which applies the mechanical deformation to the specimen through a calibrated screw, with pitch of 0.8mm, and a control electronic allows simultaneous measurement and/or control of applied load and stroke of the specimen head. The stroke is measured by a Linear Variable Differential Transformer (LVDT) while the load is measured by two miniaturized load cells with maximum capacity of 10 kN. Miniature dog bone shaped specimens with dimension showed in Fig. 4 were machined from NiTi sheets, by wire electro discharge machining, due to the poor workability of this class of materials by conventional machining processes as well as to reduce the formation of thermo-mechanical affected zone.
Step by step isothermal tensile tests were carried out, at room temperature, at increasing values of the specimen elongation. In particular, three levels of elongation have been applied, δ=0.8, 1.6 and 2.4 mm, which can be expressed as gross engineering strain (ε_g) with respect to the gauge length L_0=16 mm, *i.e.* ε_g=5, 10 and 15%. In particular, for each loading step the loading frame containing the specimen was removed from the testing machine, at fixed values of deformation, and analyzed by means of a Philips diffractometer in order to evaluate XRD spectra. XRD measurements were made with a Philips X-PERT diffractometer equipped with a vertical Bragg–Brentano powder goniometer.
A step–scan mode was used in the 20 range from 30° to 90° with a step width of 0.02° and a counting time of 2 s per step. The employed radiation was monochromated CuKα (40 kV – 40 mA). The calculation of theoretical diffractograms and the generation of structure models were performed using the PowderCell software [15].
Furthermore, the gross engineering strain has been correlated to the effective engineering strain by a finite element simulation as reported in the following section.

RESULTS AND DISUSSION

Finite Element Analyses (FEA) were carried out in order to correlate the gross engineering strain (ε_g) to the effective engineering strain (ε_e), *i.e.* to the experimentally measured engineering stress-strain curve. To this aim a 2D FE model was made, by using a commercial software, to simulate the testing conditions of the miniature specimen, and a standard non-linear solutions were adopted to model the complex stress strain behavior of the material. In particular, a quarter of the miniature specimen was modeled, due to symmetric geometry and boundary conditions,

together with a part of the loading frame, and contact conditions were defined between them in order to reproduce the testing conditions as close as possible to reality.
Gross strain is significantly greater than net strain and the difference increases when increasing the applied stress. Furthermore, this effect is also evident in the early stage of loading, i.e. in the range of elastic deformation of austenite, resulting in an apparent smaller value of the Young's modulus. This effect can be attributed to two different mechanisms: the compliance of the miniaturized testing machine and the deformation on the specimen heads. Note that a linear correction of the gross strain cannot be used here as the material non-linearity causes a marked non-linear relation between gross and net strain. For a better understanding of the results reported in the following section Fig. 3 illustrates the relation between gross strain and net strain within the range of deformation of the experiments.

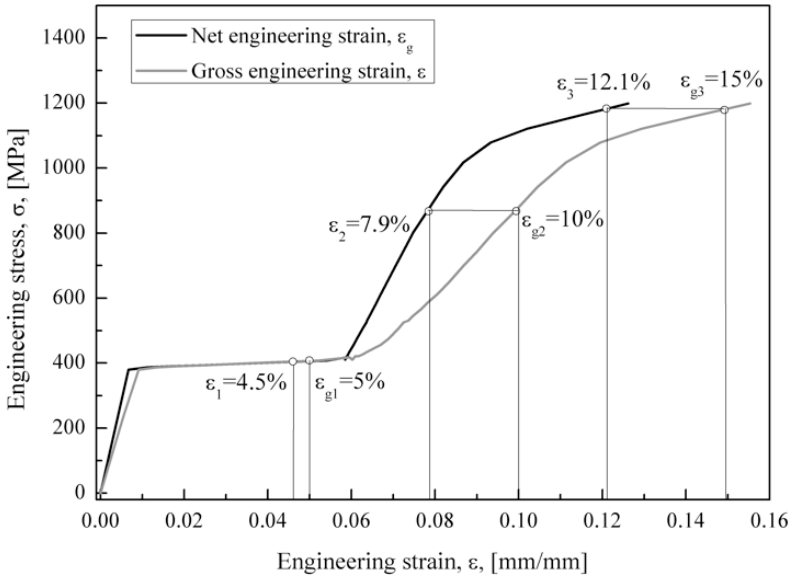

Figure 3: Relation between gross and net engineering strain obtained from FE simulations.

The first diffraction obtained in undeformed conditions, shows two peaks at 42.39 and 77.54°, corresponding to [011] and [022] crystallographic plains, typical of the austenitic phases. Using two peaks on the spectra in Fig. 4 we can evaluate the cell parameter about 3.012 Å.

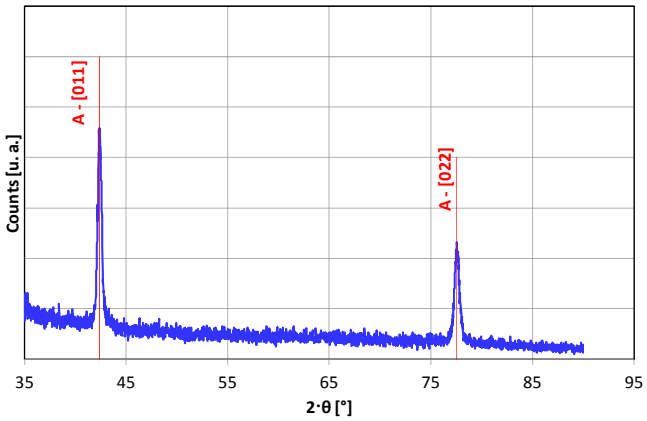

Figure 4: X-Ray spectra of the investigated NiTi alloy in stress free condition.

At the gross engineering strain ε_g=5%, corresponding to the effective engineering strain ε_e=4.5% and to a stress σ=400 MPa (Fig. 3), we can see three new peaks (42.99, 78.17 and 80.29°, as illustrated in Fig. 5a. These new peaks revealed the presence of the martensite phase which is obtained on stress plateau of the σ–ε curve.

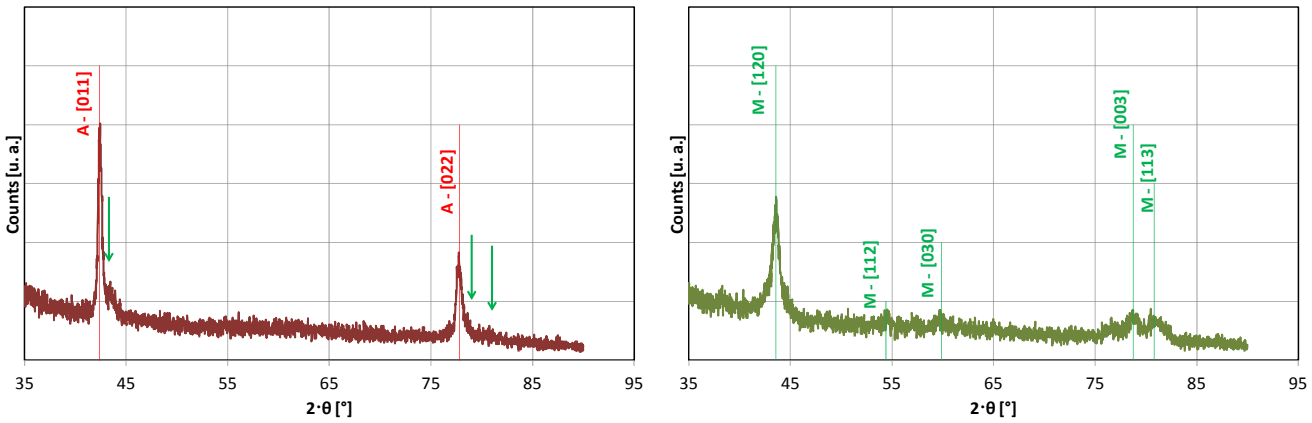

a) b)

Figure 5: X-Ray spectra of the investigated NiTi alloy: a) at ε_g=5%; b) at ε_g=10%..

Evidence of phase transition is confirmed when increasing the gross deformation up to ε_g=10%, corresponding to the effective engineering strain ε_e=7.9% and to a stress of about σ=800 MPa (Fig. 3); this loading condition corresponds to the fully transformed martensitic structure as illustrated in Fig. 5a. In this case the new phases are completely developed and their spectra are illustrated in Fig. 5b, where five peaks are observed corresponding to a monoclinic phase characterized by three cell parameters of about a=b=3.800 Å, b=2.600 Å and α=80°. The Miller indexes of the three peaks are:

- ✓ [120] for 43.55°;
- ✓ [112] for 54.39°;
- ✓ [030] for 59.90°;
- ✓ [003] for 78.72°;
- ✓ [113] for 80.80°.

The final step of the first loading cycle, consists in complete unloading, *i.e.* the applied load is removed and a final diffraction test was carried out; the corresponding spectra was compared with the initial one, as illustrated in Fig. 6a, in order to observe possible irreversible effects during loading unloading cycles. The figure shows good agreement between the two spectra, which indicates a complete recovery of initial structure. In particular, no residual martensitic structure has been observed after first cycle, confirming a good pseudo-elastic behavior of the alloy.

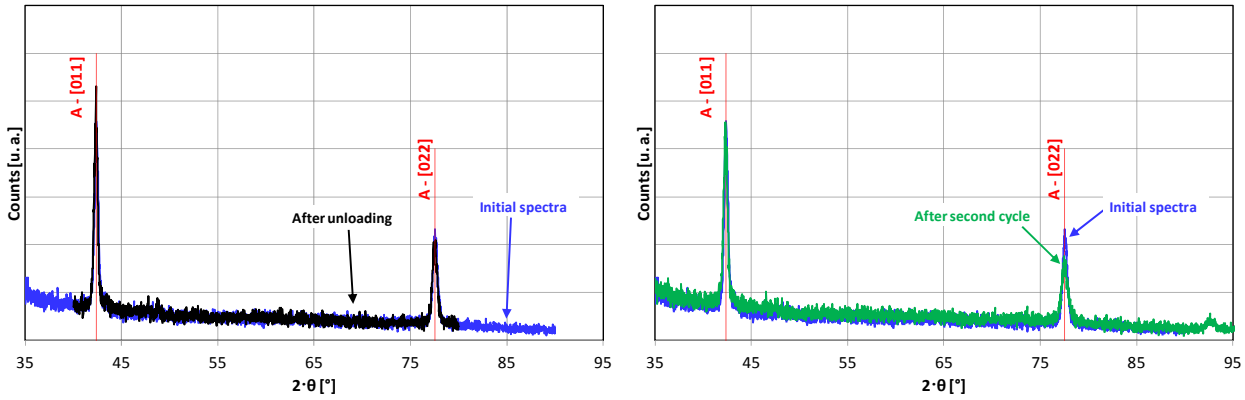

a) b)

Figure 6: Comparison of the X-Ray spectra between initial condition and final stress free condition after unloading: a) after first cycle, b) after second cycle.

Also after second cycle, no residual martensite has been observed, but Fig. 6b shows an unchanged peak at [011] and a decreased intensity of second peak at [022]. It can be assumed a relation between the strong variation of mechanical properties in first cycles and the decrease of importance of second austenite peak.

CONCLUSIONS

In this work a pseudo-elastic NiTi shape memory alloy has been investigated by using a miniaturize testing machine, which allows to analyze the microstructure evolution of the alloy at fixed values of applied load or deformations, by *in-situ* X-Ray analysis. In particular, miniaturized uniaxial specimens were used and the micro-structure evolution at increasing values of applied deformations was analyzed. The results can be summarized as follows:

- ✓ an initial cubic structure, with cell parameter of about 3.012 Å, characterizes the investigated alloy in stress free conditions; at ε=4.5%, corresponding to about σ=400 MPa in the stress plateau of the σ–ε curve, a new phase, the martensitic one, is observed; as well known the stress plateau is attributed to the transition from initial cubic structure to the new structure; at ε=7,9%, corresponding to about σ=800 MPa in the fully martensitic region of the σ–ε curve, the new structure is completely developed and the initial structure is not observed. The new structure is characterized by monoclinic cells with three cell parameters of about a=b=3.800 Å, b=2.600 Å and α=80°;
- ✓ after complete unloading the specimen recovers his initial shape and it shows the same diffraction spectra of the alloy in its initial condition; this indicate that the initial micro-structure is completely recovered without the formation of stabilized martensite;
- ✓ after second cycle a decrease intensity of second peak was observed.

REFERENCES

[1] K. Otsuka, X. Ren, Progress in Materials Science, (2005) 511.
[2] Y. Dong, Z. Boming, L. Jun, Materials Science and Engineering A, 485 (2008) 243.
[3] Y. Liu, G.S. Tan., Intermetallics, (2000) 8.
[4] Y. Liu, D. Favier, Acta Mater, (2000) 48.
[5] K.C. Russel, Phase transformation, Ohio, ASM, (1969) 1219.
[6] S. Miyazaki, M. Kimura, H. Horikawa. In: Advanced materials, K. Otsuka, Y. Fukai, editors., Amsterdam: Elsevier; 93, V/B (1994) 1097.
[7] S. Miyazaki, M. Kimura, H. Horikawa. In: Advanced materials, K. Otsuka, Y. Fukai, editors., Amsterdam: Elsevier; 93, V/B (1994) 1101.
[8] A. Sato, E. Chishima, K. Soma, T. Mori, Acta Metall, 30 (1982) 1177.
[9] K. Otsuka Shimizu, Scripta Metall, 11 (1977) 757.
[10] G.V. Kurdjumov, L.G. Khandros, Dokl Nauk SSSR, 66 (1949) 211.
[11] J.W. Christian, The theory of transformations in metals and alloys. Oxford: Pergamon Press, (1965) 815.
[12] K. Bhattacharya, S. Conti, G. Zanzotto, J. Zimmer, Nature, 428 (2004) 55.
[13] M. Pattabi, K. Ramakrishna, Materials Science and Engineering A, 486 (2008) 14.
[14] A. Undisz, M. Rettenmayr, M. Wilke, L. Spieβ, In: ESOMAT 2009, 02034 (2009), DOI:10.1051/esomat/200902034, © Owned by the authors, published by EDP Sciences (2009).
[15] PowderCell 2.3—Pulverdiffraktogramme aus Einkristalldaten und Anpassung experimenteller Beugungsaufnahmen. Available at http://www.bam.de/de/service/publikationen/powder_cell.htm.